

Measurement of the top quark mass in $p\bar{p}$ collisions at $\sqrt{s} = 1.96$ TeV using the decay length technique

A. Abulencia,²⁴ J. Adelman,¹³ T. Affolder,¹⁰ T. Akimoto,⁵⁶ M. G. Albrow,¹⁷ D. Ambrose,¹⁷ S. Amerio,⁴⁴ D. Amidei,³⁵ A. Anastassov,⁵³ K. Anikeev,¹⁷ A. Annovi,¹⁹ J. Antos,¹⁴ M. Aoki,⁵⁶ G. Apollinari,¹⁷ J.-F. Arguin,³⁴ T. Arisawa,⁵⁸ A. Artikov,¹⁵ W. Ashmanskas,¹⁷ A. Attal,⁸ F. Azfar,⁴³ P. Azzi-Bacchetta,⁴⁴ P. Azzurri,⁴⁷ N. Bacchetta,⁴⁴ W. Badgett,¹⁷ A. Barbaro-Galtieri,²⁹ V. E. Barnes,⁴⁹ B. A. Barnett,²⁵ S. Baroiant,⁷ V. Bartsch,³¹ G. Bauer,³³ F. Bedeschi,⁴⁷ S. Behari,²⁵ S. Belforte,⁵⁵ G. Bellettini,⁴⁷ J. Bellinger,⁶⁰ A. Belloni,³³ D. Benjamin,¹⁶ A. Beretvas,¹⁷ J. Beringer,²⁹ T. Berry,³⁰ A. Bhatti,⁵¹ M. Binkley,¹⁷ D. Bisello,⁴⁴ R. E. Blair,² C. Blocker,⁶ B. Blumenfeld,²⁵ A. Bocci,¹⁶ A. Bodek,⁵⁰ V. Boisvert,⁵⁰ G. Bolla,⁴⁹ A. Bolshov,³³ D. Bortoletto,⁴⁹ J. Boudreau,⁴⁸ A. Boveia,¹⁰ B. Brau,¹⁰ L. Brigliadori,⁵ C. Bromberg,³⁶ E. Brubaker,¹³ J. Budagov,¹⁵ H. S. Budd,⁵⁰ S. Budd,²⁴ S. Budroni,⁴⁷ K. Burkett,¹⁷ G. Busetto,⁴⁴ P. Bussey,²¹ K. L. Byrum,² S. Cabrera,^{16,o} M. Campanelli,²⁰ M. Campbell,³⁵ F. Canelli,¹⁷ A. Canepa,⁴⁹ S. Carillo,^{18,i} D. Carlsmith,⁶⁰ R. Carosi,⁴⁷ S. Carron,³⁴ M. Casarsa,⁵⁵ A. Castro,⁵ P. Catastini,⁴⁷ D. Cauz,⁵⁵ M. Cavalli-Sforza,³ A. Cerri,²⁹ L. Cerrito,^{43,m} S. H. Chang,²⁸ Y. C. Chen,¹ M. Chertok,⁷ G. Chiarelli,⁴⁷ G. Chlachidze,¹⁵ F. Chlebana,¹⁷ I. Cho,²⁸ K. Cho,²⁸ D. Chokheli,¹⁵ J. P. Chou,²² G. Choudalakis,³³ S. H. Chuang,⁶⁰ K. Chung,¹² W. H. Chung,⁶⁰ Y. S. Chung,⁵⁰ M. Ciljak,⁴⁷ C. I. Ciobanu,²⁴ M. A. Ciocci,⁴⁷ A. Clark,²⁰ D. Clark,⁶ M. Coca,¹⁶ G. Compostella,⁴⁴ M. E. Convery,⁵¹ J. Conway,⁷ B. Cooper,³⁶ K. Copic,³⁵ M. Cordelli,¹⁹ G. Cortiana,⁴⁴ F. Crescioli,⁴⁷ C. Cuenca Almenar,^{7,o} J. Cuevas,^{11,l} R. Culbertson,¹⁷ J. C. Cully,³⁵ D. Cyr,⁶⁰ S. DaRonco,⁴⁴ M. Datta,¹⁷ S. D'Auria,²¹ T. Davies,²¹ M. D'Onofrio,³ D. Dagenhart,⁶ P. de Barbaro,⁵⁰ S. De Cecco,⁵² A. Deisher,²⁹ G. De Lentdecker,^{50,c} M. Dell'Orso,⁴⁷ F. Delli Paoli,⁴⁴ L. Demortier,⁵¹ J. Deng,¹⁶ M. Deninno,⁵ D. De Pedis,⁵² P. F. Derwent,¹⁷ G. P. Di Giovanni,⁴⁵ C. Dionisi,⁵² B. Di Ruzza,⁵⁵ J. R. Dittmann,⁴ P. DiTuro,⁵³ C. Dörr,²⁶ S. Donati,⁴⁷ M. Donega,²⁰ P. Dong,⁸ J. Donini,⁴⁴ T. Dorigo,⁴⁴ S. Dube,⁵³ J. Efron,⁴⁰ R. Erbacher,⁷ D. Errede,²⁴ S. Errede,²⁴ R. Eusebi,¹⁷ H. C. Fang,²⁹ S. Farrington,³⁰ I. Fedorko,⁴⁷ W. T. Fedorko,¹³ R. G. Feild,⁶¹ M. Feindt,²⁶ J. P. Fernandez,³² R. Field,¹⁸ G. Flanagan,⁴⁹ A. Foland,²² S. Forrester,⁷ G. W. Foster,¹⁷ M. Franklin,²² J. C. Freeman,²⁹ I. Furic,¹³ M. Gallinaro,⁵¹ J. Galyardt,¹² J. E. Garcia,⁴⁷ F. Garbersson,¹⁰ A. F. Garfinkel,⁴⁹ C. Gay,⁶¹ H. Gerberich,²⁴ D. Gerdes,³⁵ S. Giagu,⁵² P. Giannetti,⁴⁷ A. Gibson,²⁹ K. Gibson,⁴⁸ J. L. Gimmell,⁵⁰ C. Ginsburg,¹⁷ N. Giokaris,^{15,a} M. Giordani,⁵⁵ P. Giromini,¹⁹ M. Giunta,⁴⁷ G. Giurgiu,¹² V. Glagolev,¹⁵ D. Glenzinski,¹⁷ M. Gold,³⁸ N. Goldschmidt,¹⁸ J. Goldstein,^{43,b} A. Golossanov,¹⁷ G. Gomez,¹¹ G. Gomez-Ceballos,¹¹ M. Goncharov,⁵⁴ O. González,³² I. Gorelov,³⁸ A. T. Goshaw,¹⁶ K. Goulianos,⁵¹ A. Gresele,⁴⁴ M. Griffiths,³⁰ S. Grinstein,²² C. Grosso-Pilcher,¹³ R. C. Group,¹⁸ U. Grundler,²⁴ J. Guimaraes da Costa,²² Z. Gunay-Unalan,³⁶ C. Haber,²⁹ K. Hahn,³³ S. R. Hahn,¹⁷ E. Halkiadakis,⁵³ A. Hamilton,³⁴ B.-Y. Han,⁵⁰ J. Y. Han,⁵⁰ R. Handler,⁶⁰ F. Happacher,¹⁹ K. Hara,⁵⁶ M. Hare,⁵⁷ S. Harper,⁴³ R. F. Harr,⁵⁹ R. M. Harris,¹⁷ M. Hartz,⁴⁸ K. Hatakeyama,⁵¹ J. Hauser,⁸ A. Heijboer,⁴⁶ B. Heinemann,³⁰ J. Heinrich,⁴⁶ C. Henderson,³³ M. Herndon,⁶⁰ J. Heuser,²⁶ D. Hidas,¹⁶ C. S. Hill,^{10,b} D. Hirschbuehl,²⁶ A. Hocker,¹⁷ A. Holloway,²² S. Hou,¹ M. Houlden,³⁰ S.-C. Hsu,⁹ B. T. Huffman,⁴³ R. E. Hughes,⁴⁰ U. Husemann,⁶¹ J. Huston,³⁶ J. Incandela,¹⁰ G. Introzzi,⁴⁷ M. Iori,⁵² Y. Ishizawa,⁵⁶ A. Ivanov,⁷ B. Iyutin,³³ E. James,¹⁷ D. Jang,⁵³ B. Jayatilaka,³⁵ D. Jeans,⁵² H. Jensen,¹⁷ E. J. Jeon,²⁸ S. Jindariani,¹⁸ M. Jones,⁴⁹ K. K. Joo,²⁸ S. Y. Jun,¹² J. E. Jung,²⁸ T. R. Junk,²⁴ T. Kamon,⁵⁴ P. E. Karchin,⁵⁹ Y. Kato,⁴² Y. Kemp,²⁶ R. Kephart,¹⁷ U. Kerzel,²⁶ V. Khotilovich,⁵⁴ B. Kilminster,⁴⁰ D. H. Kim,²⁸ H. S. Kim,²⁸ J. E. Kim,²⁸ M. J. Kim,¹² S. B. Kim,²⁸ S. H. Kim,⁵⁶ Y. K. Kim,¹³ N. Kimura,⁵⁶ L. Kirsch,⁶ S. Klimentenko,¹⁸ M. Klute,³³ B. Knuteson,³³ B. R. Ko,¹⁶ K. Kondo,⁵⁸ D. J. Kong,²⁸ J. Konigsberg,¹⁸ A. Korytov,¹⁸ A. V. Kotwal,¹⁶ A. Kovalev,⁴⁶ A. C. Kraan,⁴⁶ J. Kraus,²⁴ I. Kravchenko,³³ M. Kreps,²⁶ J. Kroll,⁴⁶ N. Krumnack,⁴ M. Kruse,¹⁶ V. Krutelyov,¹⁰ T. Kubo,⁵⁶ S. E. Kuhlmann,² T. Kuhr,²⁶ Y. Kusakabe,⁵⁸ S. Kwang,¹³ A. T. Laasanen,⁴⁹ S. Lai,³⁴ S. Lami,⁴⁷ S. Lammel,¹⁷ M. Lancaster,³¹ R. L. Lander,⁷ K. Lannon,⁴⁰ A. Lath,⁵³ G. Latino,⁴⁷ I. Lazzizzera,⁴⁴ T. LeCompte,² J. Lee,⁵⁰ J. Lee,²⁸ Y. J. Lee,²⁸ S. W. Lee,^{54,n} R. Lefèvre,³ N. Leonardo,³³ S. Leone,⁴⁷ S. Levy,¹³ J. D. Lewis,¹⁷ C. Lin,⁶¹ C. S. Lin,¹⁷ M. Lindgren,¹⁷ E. Lipeles,⁹ A. Lister,⁷ D. O. Litvintsev,¹⁷ T. Liu,¹⁷ N. S. Lockyer,⁴⁶ A. Loginov,⁶¹ M. Loreti,⁴⁴ P. Loverre,⁵² R.-S. Lu,¹ D. Lucchesi,⁴⁴ P. Lujan,²⁹ P. Lukens,¹⁷ G. Lungu,¹⁸ L. Lyons,⁴³ J. Lys,²⁹ R. Lysak,¹⁴ E. Lytken,⁴⁹ P. Mack,²⁶ D. MacQueen,³⁴ R. Madrak,¹⁷ K. Maeshima,¹⁷ K. Makhoul,³³ T. Maki,²³ P. Maksimovic,²⁵ S. Malde,⁴³ G. Manca,³⁰ F. Margaroli,⁵ R. Marginean,¹⁷ C. Marino,²⁶ C. P. Marino,²⁴ A. Martin,⁶¹ M. Martin,²¹ V. Martin,^{21,g} M. Martínez,³ T. Maruyama,⁵⁶ P. Mastrandrea,⁵² T. Masubuchi,⁵⁶ H. Matsunaga,⁵⁶ M. E. Mattson,⁵⁹ R. Mazini,³⁴ P. Mazzanti,⁵ K. S. McFarland,⁵⁰ P. McIntyre,⁵⁴ R. McNulty,^{30,f} A. Mehta,³⁰ P. Mehtala,²³ S. Menzemer,^{11,h} A. Menzione,⁴⁷ P. Merkel,⁴⁹ C. Mesropian,⁵¹ A. Messina,³⁶ T. Miao,¹⁷ N. Miladinovic,⁶ J. Miles,³³ R. Miller,³⁶ C. Mills,¹⁰ M. Milnik,²⁶ A. Mitra,¹ G. Mitselmakher,¹⁸ A. Miyamoto,²⁷ S. Moed,²⁰ N. Moggi,⁵ B. Mohr,⁸ R. Moore,¹⁷ M. Morello,⁴⁷ P. Movilla Fernandez,²⁹ J. Mülmenstädt,²⁹ A. Mukherjee,¹⁷ Th. Muller,²⁶ R. Mumford,²⁵ P. Murat,¹⁷ J. Nachtman,¹⁷

A. Nagano,⁵⁶ J. Naganoma,⁵⁸ I. Nakano,⁴¹ A. Napier,⁵⁷ V. Necula,¹⁸ C. Neu,⁴⁶ M. S. Neubauer,⁹ J. Nielsen,²⁹ T. Nigmanov,⁴⁸ L. Nodulman,² O. Normiella,³ E. Nurse,³¹ S. H. Oh,¹⁶ Y. D. Oh,²⁸ I. Oksuzian,¹⁸ T. Okusawa,⁴² R. Oldeman,³⁰ R. Orava,²³ K. Osterberg,²³ C. Pagliarone,⁴⁷ E. Palencia,¹¹ V. Papadimitriou,¹⁷ A. A. Paramonov,¹³ B. Parks,⁴⁰ S. Pashapour,³⁴ J. Patrick,¹⁷ G. Pauletta,⁵⁵ M. Paulini,¹² C. Paus,³³ D. E. Pellett,⁷ A. Penzo,⁵⁵ T. J. Phillips,¹⁶ G. Piacentino,⁴⁷ J. Piedra,⁴⁵ L. Pinera,¹⁸ K. Pitts,²⁴ C. Plager,⁸ L. Pondrom,⁶⁰ X. Portell,³ O. Poukhov,¹⁵ N. Pounder,⁴³ F. Prakoshyn,¹⁵ A. Pronko,¹⁷ J. Proudfoot,² F. Ptohos,^{19,e} G. Punzi,⁴⁷ J. Pursley,²⁵ J. Rademacker,^{43,b} A. Rahaman,⁴⁸ N. Ranjan,⁴⁹ S. Rappoccio,²² B. Reisert,¹⁷ V. Rekovic,³⁸ P. Renton,⁴³ M. Rescigno,⁵² S. Richter,²⁶ F. Rimondi,⁵ L. Ristori,⁴⁷ A. Robson,²¹ T. Rodrigo,¹¹ E. Rogers,²⁴ S. Rolli,⁵⁷ R. Roser,¹⁷ M. Rossi,⁵⁵ R. Rossin,¹⁸ A. Ruiz,¹¹ J. Russ,¹² V. Rusu,¹³ H. Saarikko,²³ S. Sabik,³⁴ A. Safonov,⁵⁴ W. K. Sakumoto,⁵⁰ G. Salamanna,⁵² O. Saltó,³ D. Saltzberg,⁸ C. Sánchez,³ L. Santi,⁵⁵ S. Sarkar,⁵² L. Sartori,⁴⁷ K. Sato,¹⁷ P. Savard,³⁴ A. Savoy-Navarro,⁴⁵ T. Scheidle,²⁶ P. Schlabach,¹⁷ E. E. Schmidt,¹⁷ M. P. Schmidt,⁶¹ M. Schmitt,³⁹ T. Schwarz,⁷ L. Scodellaro,¹¹ A. L. Scott,¹⁰ A. Scribano,⁴⁷ F. Scuri,⁴⁷ A. Sedov,⁴⁹ S. Seidel,³⁸ Y. Seiya,⁴² A. Semenov,¹⁵ L. Sexton-Kennedy,¹⁷ A. Sfyrla,²⁰ M. D. Shapiro,²⁹ T. Shears,³⁰ P. F. Shepard,⁴⁸ D. Sherman,²² M. Shimojima,^{56,k} M. Shochet,¹³ Y. Shon,⁶⁰ I. Shreyber,³⁷ A. Sidoti,⁴⁷ P. Sinervo,³⁴ A. Sisakyan,¹⁵ J. Sjolin,⁴³ A. J. Slaughter,¹⁷ J. Slaunwhite,⁴⁰ K. Sliwa,⁵⁷ J. R. Smith,⁷ F. D. Snider,¹⁷ R. Snihur,³⁴ M. Soderberg,³⁵ A. Soha,⁷ S. Somalwar,⁵³ V. Sorin,³⁶ J. Spalding,¹⁷ F. Spinella,⁴⁷ T. Spreitzer,³⁴ P. Squillacioti,⁴⁷ M. Stanitzki,⁶¹ A. Staveris-Polykalas,⁴⁷ R. St. Denis,²¹ B. Stelzer,⁸ O. Stelzer-Chilton,⁴³ D. Stentz,³⁹ J. Strologas,³⁸ D. Stuart,¹⁰ J. S. Suh,²⁸ A. Sukhanov,¹⁸ H. Sun,⁵⁷ T. Suzuki,⁵⁶ A. Taffard,²⁴ R. Takashima,⁴¹ Y. Takeuchi,⁵⁶ K. Takikawa,⁵⁶ M. Tanaka,² R. Tanaka,⁴¹ M. Tecchio,³⁵ P. K. Teng,¹ K. Terashi,⁵¹ J. Thom,^{17,d} A. S. Thompson,²¹ E. Thomson,⁴⁶ P. Tipton,⁶¹ V. Tiwari,¹² S. Tkaczyk,¹⁷ D. Toback,⁵⁴ S. Tokar,¹⁴ K. Tollefson,³⁶ T. Tomura,⁵⁶ D. Tonelli,⁴⁷ S. Torre,¹⁹ D. Torretta,¹⁷ S. Tourneur,⁴⁵ W. Trischuk,³⁴ R. Tsuchiya,⁵⁸ S. Tsuno,⁴¹ N. Turini,⁴⁷ F. Ukegawa,⁵⁶ T. Unverhau,²¹ S. Uozumi,⁵⁶ D. Usynin,⁴⁶ S. Vallecorsa,²⁰ N. van Remortel,²³ A. Varganov,³⁵ E. Vataga,³⁸ F. Vázquez,^{18,i} G. Velev,¹⁷ G. Veramendi,²⁴ V. Veszpremi,⁴⁹ R. Vidal,¹⁷ I. Vila,¹¹ R. Vilar,¹¹ T. Vine,³¹ I. Vollrath,³⁴ I. Volobouev,^{29,n} G. Volpi,⁴⁷ F. Würthwein,⁹ P. Wagner,⁵⁴ R. G. Wagner,² R. L. Wagner,¹⁷ J. Wagner,²⁶ W. Wagner,²⁶ R. Wallny,⁸ S. M. Wang,¹ A. Warburton,³⁴ S. Waschke,²¹ D. Waters,³¹ M. Weinberger,⁵⁴ W. C. Wester III,¹⁷ B. Whitehouse,⁵⁷ D. Whiteson,⁴⁶ A. B. Wicklund,² E. Wicklund,¹⁷ G. Williams,³⁴ H. H. Williams,⁴⁶ P. Wilson,¹⁷ B. L. Winer,⁴⁰ P. Wittich,^{17,d} S. Wolbers,¹⁷ C. Wolfe,¹³ T. Wright,³⁵ X. Wu,²⁰ S. M. Wynne,³⁰ A. Yagil,¹⁷ K. Yamamoto,⁴² J. Yamaoka,⁵³ T. Yamashita,⁴¹ C. Yang,⁶¹ U. K. Yang,^{13,j} Y. C. Yang,²⁸ W. M. Yao,²⁹ G. P. Yeh,¹⁷ J. Yoh,¹⁷ K. Yorita,¹³ T. Yoshida,⁴² G. B. Yu,⁵⁰ I. Yu,²⁸ S. S. Yu,¹⁷ J. C. Yun,¹⁷ L. Zanello,⁵² A. Zanetti,⁵⁵ I. Zaw,²² X. Zhang,²⁴ J. Zhou,⁵³ and S. Zucchelli⁵

(CDF Collaboration)^a¹*Institute of Physics, Academia Sinica, Taipei, Taiwan 11529, Republic of China*²*Argonne National Laboratory, Argonne, Illinois 60439, USA*³*Institut de Física d'Altes Energies, Universitat Autònoma de Barcelona, E-08193, Bellaterra (Barcelona), Spain*⁴*Baylor University, Waco, Texas 76798, USA*⁵*Istituto Nazionale di Fisica Nucleare, University of Bologna, I-40127 Bologna, Italy*⁶*Brandeis University, Waltham, Massachusetts 02254, USA*⁷*University of California, Davis, Davis, California 95616, USA*⁸*University of California, Los Angeles, Los Angeles, California 90024, USA*⁹*University of California, San Diego, La Jolla, California 92093, USA*¹⁰*University of California, Santa Barbara, Santa Barbara, California 93106, USA*¹¹*Instituto de Física de Cantabria, CSIC-University of Cantabria, 39005 Santander, Spain*¹²*Carnegie Mellon University, Pittsburgh, Pennsylvania 15213, USA*¹³*Enrico Fermi Institute, University of Chicago, Chicago, Illinois 60637, USA*¹⁴*Comenius University, 842 48 Bratislava, Slovakia; Institute of Experimental Physics, 040 01 Kosice, Slovakia*¹⁵*Joint Institute for Nuclear Research, RU-141980 Dubna, Russia*¹⁶*Duke University, Durham, North Carolina 27708*¹⁷*Fermi National Accelerator Laboratory, Batavia, Illinois 60510, USA*¹⁸*University of Florida, Gainesville, Florida 32611, USA*¹⁹*Laboratori Nazionali di Frascati, Istituto Nazionale di Fisica Nucleare, I-00044 Frascati, Italy*²⁰*University of Geneva, CH-1211 Geneva 4, Switzerland*²¹*Glasgow University, Glasgow G12 8QQ, United Kingdom*²²*Harvard University, Cambridge, Massachusetts 02138, USA*²³*Division of High Energy Physics, Department of Physics, University of Helsinki and Helsinki Institute of Physics, FIN-00014, Helsinki, Finland*

- ²⁴University of Illinois, Urbana, Illinois 61801, USA
²⁵The Johns Hopkins University, Baltimore, Maryland 21218, USA
²⁶Institut für Experimentelle Kernphysik, Universität Karlsruhe, 76128 Karlsruhe, Germany
²⁷High Energy Accelerator Research Organization (KEK), Tsukuba, Ibaraki 305, Japan
²⁸Center for High Energy Physics: Kyungpook National University, Taegu 702-701, Korea;
 Seoul National University, Seoul 151-742, Korea;
 and SungKyunKwan University, Suwon 440-746, Korea
²⁹Ernest Orlando Lawrence Berkeley National Laboratory, Berkeley, California 94720, USA
³⁰University of Liverpool, Liverpool L69 7ZE, United Kingdom
³¹University College London, London WC1E 6BT, United Kingdom
³²Centro de Investigaciones Energeticas Medioambientales y Tecnologicas, E-28040 Madrid, Spain
³³Massachusetts Institute of Technology, Cambridge, Massachusetts 02139, USA
³⁴Institute of Particle Physics: McGill University, Montréal, Canada H3A 2T8;
 and University of Toronto, Toronto, Canada M5S 1A7
³⁵University of Michigan, Ann Arbor, Michigan 48109, USA
³⁶Michigan State University, East Lansing, Michigan 48824, USA
³⁷Institution for Theoretical and Experimental Physics, ITEP, Moscow 117259, Russia
³⁸University of New Mexico, Albuquerque, New Mexico 87131, USA
³⁹Northwestern University, Evanston, Illinois 60208, USA
⁴⁰The Ohio State University, Columbus, Ohio 43210, USA
⁴¹Okayama University, Okayama 700-8530, Japan
⁴²Osaka City University, Osaka 588, Japan
⁴³University of Oxford, Oxford OX1 3RH, United Kingdom
⁴⁴University of Padova, Istituto Nazionale di Fisica Nucleare, Sezione di Padova-Trento, I-35131 Padova, Italy
⁴⁵LPNHE, Universite Pierre et Marie Curie/IN2P3-CNRS, UMR7585, Paris, F-75252 France
⁴⁶University of Pennsylvania, Philadelphia, Pennsylvania 19104, USA
⁴⁷Istituto Nazionale di Fisica Nucleare Pisa, Universities of Pisa, Siena
 and Scuola Normale Superiore, I-56127 Pisa, Italy
⁴⁸University of Pittsburgh, Pittsburgh, Pennsylvania 15260, USA
⁴⁹Purdue University, West Lafayette, Indiana 47907, USA
⁵⁰University of Rochester, Rochester, New York 14627, USA
⁵¹The Rockefeller University, New York, New York 10021, USA
⁵²Istituto Nazionale di Fisica Nucleare, Sezione di Roma 1, University of Rome "La Sapienza," I-00185 Roma, Italy
⁵³Rutgers University, Piscataway, New Jersey 08855, USA
⁵⁴Texas A&M University, College Station, Texas 77843, USA
⁵⁵Istituto Nazionale di Fisica Nucleare, University of Trieste/ Udine, Italy
⁵⁶University of Tsukuba, Tsukuba, Ibaraki 305, Japan
⁵⁷Tufts University, Medford, Massachusetts 02155, USA
⁵⁸Waseda University, Tokyo 169, Japan
⁵⁹Wayne State University, Detroit, Michigan 48201, USA
⁶⁰University of Wisconsin, Madison, Wisconsin 53706, USA
⁶¹Yale University, New Haven, Connecticut 06520, USA
 (Received 24 December 2006; published 10 April 2007)

We report the first measurement of the top quark mass using the decay length technique in $p\bar{p}$ collisions at a center-of-mass energy of 1.96 TeV. This technique uses the measured flight distance of the b hadron to

- ^aVisiting scientist from University of Athens, 157 84 Athens, Greece
^bVisiting scientist from University of Bristol, Bristol BS8 1TL, United Kingdom
^cVisiting scientist from Universite Libre de Bruxelles (ULB), B-1050 Brussels, Belgium
^dVisiting scientist from Cornell University, Ithaca, NY 14853, USA
^eVisiting scientist from University of Cyprus, Nicosia CY-1678, Cyprus
^fVisiting scientist from University College Dublin, Dublin 4, Ireland
^gVisiting scientist from University of Edinburgh, Edinburgh EH9 3JZ, United Kingdom
^hVisiting scientist from University of Heidelberg, D-69120 Heidelberg, Germany
ⁱVisiting scientist from University of Iberoamericana, Mexico D.F., Mexico
^jVisiting scientist from University of Manchester, Manchester M13 9PL, United Kingdom
^kVisiting scientist from Nagasaki Institute of Applied Science, Nagasaki, Japan
^lVisiting scientist from Universidad de Oviedo, E-33007 Oviedo, Spain
^mVisiting scientist from Queen Mary and Westfield College, London, E1 4NS, United Kingdom
ⁿVisiting scientist from Texas Tech University, Lubbock, TX 79409, USA
^oVisiting scientist from Instituto de Fisica Corpuscular (IFIC), 46071 Valencia, Spain

infer the mass of the top quark in lepton plus jets events with missing transverse energy. It relies solely on tracking and avoids the jet energy scale uncertainty that is common to all other methods used so far. We apply our novel method to a 695 pb^{-1} data sample recorded by the CDF II detector at Fermilab and extract a measurement of $m_t = 180.7_{-13.4}^{+15.5}(\text{stat.}) \pm 8.6(\text{sys.}) \text{ GeV}/c^2$. While the uncertainty of this result is larger than that of other measurements, the dominant uncertainties in the decay length technique are uncorrelated with those in other methods. This result can help reduce the overall uncertainty when combined with other existing measurements of the top quark mass.

DOI: [10.1103/PhysRevD.75.071102](https://doi.org/10.1103/PhysRevD.75.071102)

PACS numbers: 14.65.Ha, 12.15.Ff

A precise determination of the top quark mass (m_t) is an important goal of high-energy physics. The uncertainty on m_t is a dominant uncertainty in global standard model (SM) fits for the mass of the unobserved Higgs boson. Recently, significant progress has been made in reducing the uncertainty in measurements of m_t [1]. Unfortunately, the most precise of the current techniques are all limited by the same systematic uncertainty, the calorimeter jet energy scale.

We have developed a novel method to measure m_t using the transverse decay length of b hadrons from top decays [2]. The method exploits the fact that top quarks produced in $p\bar{p}$ collisions at $\sqrt{s} = 1.96 \text{ TeV}$ are nearly at rest and decay almost instantaneously [3] to a relatively light b quark and a much heavier W boson. In the rest frame of the top quark, the b quark Lorentz factor is:

$$\gamma_b = \frac{m_t^2 + m_b^2 - m_W^2}{2m_t m_b} \approx 0.4 \frac{m_t}{m_b} \quad (1)$$

where $\gamma_b \equiv [1 - (v_b^2/c^2)]^{-1/2}$ and the approximation makes use of the fact that $m_t \gg m_b$ and $m_W^2 \approx 0.2m_t^2$. The mass of the top quark, therefore, is strongly correlated with the velocity imparted to the b quark and the subsequent b hadron after fragmentation. Thus, the average momentum of the b hadrons from top decays can be used to infer m_t . Rather than measuring the average momentum, we measure the highly-correlated average transverse decay length of the b hadrons, which we denote $\langle L_{2D} \rangle$. Furthermore, we do not analytically solve for m_t from $\langle L_{2D} \rangle$; we establish the functional dependence of m_t on $\langle L_{2D} \rangle$ using Monte Carlo (MC) simulations of signal and background events.

This technique relies on track reconstruction to determine precisely the decay length. The calorimeter information is used only for the selection of event candidates. Consequently, the uncertainty on the measurement due to the jet energy scale is negligible. In this paper, we present the first measurement of m_t using the decay length technique. We apply this method to $p\bar{p}$ collision data recorded by the CDF II detector during Run II of the Fermilab Tevatron. CDF II is a general purpose particle physics detector and is described in detail elsewhere [4].

Run II of the Tevatron collides $p\bar{p}$ beams at $\sqrt{s} = 1.96 \text{ TeV}$. In such collisions, $t\bar{t}$ pairs are produced predominantly through $q\bar{q}$ annihilation. Top quarks decay almost exclusively to a W boson and a b quark. The W

subsequently decays either hadronically, to a pair of quarks or leptonically, to a lepton and a neutrino. The final state $b\bar{b}\ell\bar{\nu}q\bar{q}'$ (where $\ell = e, \mu$ only) resulting from one of each type of W decay is called the “lepton + jets” mode. This channel has a large branching fraction with a good signal-to-background ratio; we use it to measure m_t using the decay length technique. Lepton + jets $t\bar{t}$ events typically contain a high transverse momentum (p_T) electron or muon, missing transverse energy (\cancel{E}_T) from the undetected neutrino, and four high transverse energy (E_T) jets, two of which originate from b quarks [5]. Traditional measurements of m_t require all four jets, since they fully reconstruct the top quark decays. Sometimes a jet may not be reconstructed, making those events ineligible for these methods. The decay length technique, however, can be applied to such events, providing the only measurement of m_t from these data.

Results reported here are obtained from an analysis of a data sample corresponding to an integrated luminosity of $\approx 695 \text{ pb}^{-1}$. From an inclusive lepton dataset we select events with an electron (muon) with $E_T > 20 \text{ GeV}$ ($p_T > 20 \text{ GeV}/c$), $\cancel{E}_T > 20 \text{ GeV}$, and at least 3 jets with $|\eta| < 2$ and energy-corrected [6] $E_T > 15 \text{ GeV}$ [7]. Electron candidates are required to have a well-measured track pointing at an isolated energy deposit in the calorimeter, and must have shower profiles consistent with expectation. We select muon candidates by requiring that the energy deposited in the calorimeters is consistent with that of a minimum ionizing particle. In addition, we match partially reconstructed tracks in the muon chambers with well-measured tracks reconstructed in the drift chamber. Jets are clustered using a fixed-cone algorithm with a cone size $\Delta R \equiv \sqrt{(\Delta\eta)^2 + (\Delta\phi)^2} = 0.4$. Finally, in order to better distinguish $t\bar{t}$ events from background processes, we require at least one jet in the event to be identified as a b jet (“positively tagged”) by the reconstruction of a secondary vertex within that jet as described below. The above selection results in 375 events with 456 positively tagged jets. We refer to this as the “positively tagged lepton + jets” sample.

The primary (PRIMEVTX) and secondary (SECVTX) vertex algorithms used are described in Ref. [8]. PRIMEVTX reconstructs the primary event vertex with a precision of $\approx 15 \mu\text{m}$ in the plane transverse to the beam for $t\bar{t}$ events. SECVTX exploits the relatively long lifetime of b hadrons in top decays to reconstruct a secondary vertex significantly

displaced from the primary interaction. Secondary vertex tagging operates on a per-jet basis, where only tracks associated with the jet are considered. We require that these tracks include at least three $r - \phi$ measurements in the silicon vertex detector, are within 2.0 cm from the primary vertex in the longitudinal direction, and that the final track fits have $\chi^2/\text{d.o.f.} \leq 8.0$. We select tracks contained inside a jet which are displaced with respect to the primary vertex if they have a large well-measured impact parameter with respect to that same vertex. The SECVTX algorithm uses a two-pass approach to find secondary vertices from these selected tracks. In the first pass, it attempts to reconstruct a secondary vertex which includes at least three tracks. If the first pass is unsuccessful, a second pass is attempted which makes tighter track requirements and tries to reconstruct a two-track vertex.

Once a secondary vertex is found, we calculate L_{2D} as the projection onto the jet axis, in the plane transverse to the beam, of the vector pointing from the primary vertex to the secondary vertex. The sign of L_{2D} is given by the ϕ difference between the jet axis and the secondary vertex vector (positive if less than 90° , negative if greater than 90°). The secondary vertices corresponding to the decay of b and c hadrons have large positive L_{2D} , while the secondary vertices from mismeasured tracks form a Gaussian distribution centered around $L_{2D} = 0$ with a width corresponding to the detector resolution. A jet is ‘‘positively tagged’’ if its transverse decay length divided by the uncertainty on that measurement ($L_{2D}/\sigma_{L_{2D}}$) is greater than 7.5. Similarly, a jet is ‘‘negatively tagged’’ if $L_{2D}/\sigma_{L_{2D}} < -7.5$. The positively tagged jet sample is predominantly composed of heavy-flavor (b or c) jets while the negatively tagged sample is mostly composed of light quark jets.

This analysis requires an accurate simulation of L_{2D} . To check the accuracy of the CDF II simulation we examine dijet data samples containing an electron (muon) with $E_T(p_T) \geq 8$ GeV. The lepton in these data often comes from the semileptonic decay of a b or c quark such that the heavy-flavor content of these samples is enhanced relative to generic dijet data. We compare these to HERWIG [9] generic dijet MC samples which have been preselected to also contain such a lepton. To increase the $b\bar{b}$ purity of these samples, we require that the lepton be contained within a jet with $E_T > 9$ GeV that is also positively tagged by SECVTX. We also require the presence of another jet with $E_T > 9$ GeV and $\Delta\phi > 2.0$ that is also positively tagged. Finally, in order to distinguish b quarks from c quarks, we require the invariant mass of the four-vectors forming the secondary vertex [10] of the tagged jets to be greater than 1.5 GeV/ c^2 . With this selection, a purity of $\approx 99\%b\bar{b}$ is obtained [11]. For all events passing the selection criteria, we make a histogram of the L_{2D} for all positive tags. These histograms are shown with observed data and MC overlaid in Fig. 1.

We observe that the simulation models the L_{2D} distribution very well. We quantify this agreement by measuring

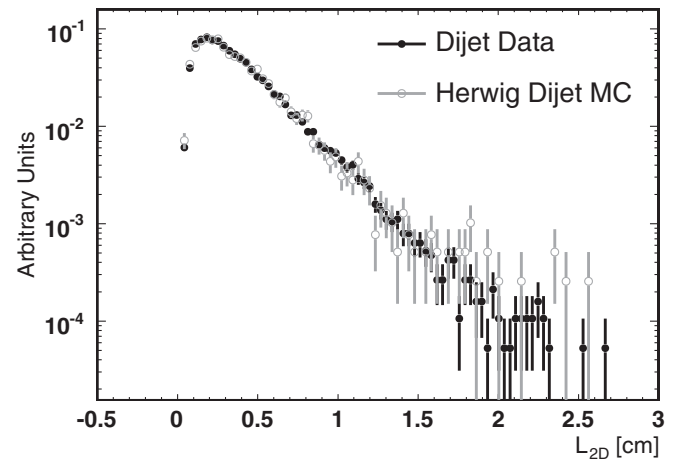


FIG. 1. Comparison of L_{2D} of positive tags from observed data and dijet MC in events with two SECVTX tags and an identified electron or muon in one of the two tagged jets. Both the lepton tag and the nonlepton tag are included. Both distributions are normalized to unit area.

$\langle L_{2D} \rangle$ for both observed data and MC, $\langle L_{2D}^{\text{data}} \rangle = 0.378 \pm 0.002$ cm and $\langle L_{2D}^{\text{MC}} \rangle = 0.381 \pm 0.004$ cm, respectively. From these, we compute a data/MC scale factor which could be applied to the $\langle L_{2D} \rangle$ measured in the observed data of 0.992 ± 0.012 . This number is consistent with a scale factor of unity; we conclude that our simulation models the L_{2D} of b hadrons with sufficient accuracy and do not apply any correction to the observed data. This ratio encompasses many different possible sources of discrepancy between our observed data and our MC simulation including effects from detector resolution, fragmentation, and the relative proportions and lifetimes of the various b hadrons. It is a comprehensive data-driven means of quantifying any systematic uncertainties in the measurement of $\langle L_{2D} \rangle$. We note that in order to apply this treatment to b hadrons in $t\bar{t}$ events, we rely on the assumption of the universality of b -fragmentation, i.e. that the fragmentation of a b quark is independent of the process in which that b quark was produced. This assumption is predicted by the QCD factorization theorem [12] and is supported by a significant body of experimental evidence [13]. We assign the 1.2% statistical uncertainty on the central value in the above calculation as a systematic uncertainty on the accuracy of our MC simulation.

We perform several additional checks on the data/MC scale factor. Since the average energy of b hadrons from top decays is higher than that of those used to compute the scale factor, we examine the ratio as a function of jet E_T . We find the scale factor to be independent of jet energy within uncertainties. We also compute a data/MC ratio of the $\langle L_{2D} \rangle$ for negatively tagged jets, thereby cross-checking the resolution modeling of the simulation. We again measure a scale factor of unity within uncertainties.

The positively tagged lepton + jets sample selected as described above has an expected signal-to-background

ratio of about 2.5:1. The dominant background is the production of W plus multijet events. These events enter the signal sample when one of the jets is a b jet or c jet, or a light quark jet that has been mistakenly tagged as containing a secondary vertex. We call the latter type of events “mistags.” The other substantial background comes from collisions which do not produce a W boson, termed “non- W ” events. These events are typically QCD multijet events where one jet has been misidentified as a high- p_T lepton and mismeasured energies produce apparent \cancel{E}_T . Additionally, other processes such as WW , WZ , ZZ , $Z \rightarrow \tau\tau$, and single top contribute small amounts to the positively tagged lepton + jet sample. The techniques used to calculate the expected contributions to this sample are detailed elsewhere [8]. Estimated contributions to the positively tagged lepton + jets sample are summarized in Table I.

We generate HERWIG $t\bar{t}$ MC samples using the CTEQ5L parton distribution functions [14] followed by a detailed simulation of the CDF II detector. The CLEO QQ MC simulation [15] models the decays of b and c hadrons. We produce these samples with top quark masses ranging from 130–230 GeV/ c^2 in 5 GeV/ c^2 intervals. We subject these simulated events to the identical event selection as that required of the observed data. After selection, we obtain L_{2D} distributions for all positive tags for each mass point. A similar process is performed for each of the backgrounds described above. We model the L_{2D} distributions for the $Wb\bar{b}$, $Wc\bar{c}$, and Wc backgrounds using ALPGEN [16] matrix element calculations which have been interfaced with HERWIG to simulate the hadronization process. To model the L_{2D} distribution from the W + mistag background we construct a hybrid data/MC template. Mistags can either come from tracks which appear displaced due to limited impact-parameter resolution or from tracks that originate from actual long-lived particles that

TABLE I. Estimated number of events from background sources and single top that contribute to the positively tagged lepton + jets sample. The excess of observed data above the total background plus single top is assumed to be $t\bar{t}$ events. Errors include statistical and systematic uncertainties.

Source	Number of Events
$Wb\bar{b}$	27.9 ± 6.2
$Wc\bar{c}$	12.2 ± 3.2
Wc	6.9 ± 1.6
non- W	12.5 ± 2.6
Mistags	40.9 ± 3.8
$WW, WZ, ZZ, Z \rightarrow \tau\tau$	5.7 ± 1.0
Total Background	106.1 ± 10.5
Single Top	5.3 ± 0.5
Total Background + Single Top	111.4 ± 11.0
Observed Data	375

are not b hadrons. We use tags from negatively tagged W + jets data, reflected about $L_{2D} = 0$, to obtain a data-driven positive mistag shape to model the resolution contribution to the distribution. We combine this with ALPGEN interfaced to HERWIG MC simulations of W + multijets, which we rely on to model the contribution from long-lived particles such as K_S and Λ . We obtain the relative normalization for this combination from independent studies comparing positive and negative tags [8]. For the purpose of this analysis, WW , WZ , ZZ , $Z \rightarrow \tau\tau$ events are considered mistags, and the mistag L_{2D} distribution obtained above is used to model their small contribution. We obtain the non- W background L_{2D} distribution directly from our observed data. We select events with identical criteria to those for the signal sample, except that we invert the requirement that the lepton be calorimetrically isolated. For most top analyses, single top is a background to the pair-produced signal. With the decay length technique, however, this is not the case. Although the correlation is not as strong as for pair-produced top quarks [17], the $\langle L_{2D} \rangle$ from b hadrons from single top decays is also correlated with m_t . We use PYTHIA [18] MC to model the single-top L_{2D} distribution as a function of m_t from 130–230 GeV/ c^2 .

As a cross-check on the modeling of L_{2D} for the various background processes, we compare the L_{2D} distribution observed in background-dominated one- and two-jet events in the lepton + jet sample with the expected signal and background contributions. Good agreement between MC and experimental data is observed; a Kolmogorov–Smirnov (KS) test yields a p -value of 30.6%.

We treat the signal and background L_{2D} distributions described above as probability density functions from which we form ensembles of simulated experiments. In forming each ensemble, the number of events from a given background source (and single top) is obtained by allowing the number of events for each process to fluctuate separately about the expected contributions listed in Table I. The number of events from $t\bar{t}$, which is similarly allowed to fluctuate, is taken to be the excess of the observed data in the positively tagged lepton + jets sample over the summed contributions of the background processes and single top production.

In computing $\langle L_{2D} \rangle$, we sum over tags rather than events. We convert the number of events for each process to a number of tags by multiplying by the probability, obtained from MC simulation, for that process to contain more than one SECVTX tags. We repeat this procedure 1000 times for each mass point over the full mass range 130–230 GeV/ c^2 . We construct histograms of the $\langle L_{2D} \rangle$ that results from each pseudoexperiment performed at a given m_t . We extract the mean and $\pm 1\sigma$ variance from these histograms, for each value of m_t , and fit these points to third-degree polynomials. The fit to the mean establishes the most probable value for a true m_t given a measured $\langle L_{2D} \rangle$ and is the

function used to make the m_t measurement from the $\langle L_{2D} \rangle$ observed in the data. Similarly, the fits to the variance form $\pm 1\sigma$ Neyman [19] confidence intervals which is used to give the statistical uncertainty of the measurement are shown in Fig. 2.

We derived these functions and validated our method prior to examining our experimental data. We employed simulated data ensembles containing MC $t\bar{t}$ events with unknown top quark mass to demonstrate that m_t could be extracted accurately and with appropriate precision.

The systematic uncertainties for this measurement come from three kinds of sources. The first arises from the accuracy of the modeling of factors which affect the top (or subsequent b) quark's momentum. We estimate the uncertainty due to initial- and final-state gluon radiation by varying the relevant parameters by $\pm 1\sigma$ in the simulation [20] and observing the effect on the measured m_t . We quote half the difference between these variations as the systematic uncertainty (1.0 and 0.9 GeV/ c^2 , respectively). To assess the systematic uncertainty from our choice of the CTEQ5L parton distribution function, we observe the shift in m_t that results when we substitute the MRST72 and MRST75 sets [21] which are evaluated at different values of the strong coupling constant, α_s . Additionally, we vary the 20 eigenvectors in the CTEQ6M package [22] by ± 100 units in χ^2 . We add the shifts observed in m_t in quadrature to determine a combined systematic uncertainty of 0.5 GeV/ c^2 . We estimate the systematic uncertainty due to our choice of HERWIG to simulate our signal events to be 0.7 GeV/ c^2 by measuring the shift induced in m_t upon substitution of PYTHIA simulations. Finally, we evaluate the uncertainty due to the jet energy scale by applying jet energy corrections which have been shifted by $\pm 1\sigma$ [7] and taking half the difference as a systematic error of 0.3 GeV/ c^2 . As anticipated, we find the analysis to have negligible sensitivity to such shifts.

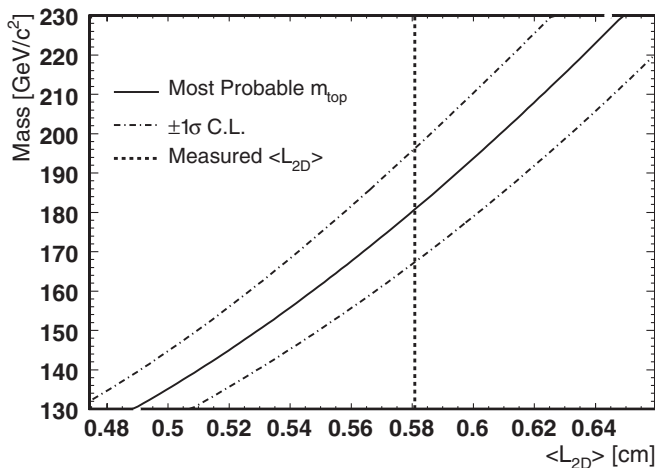


FIG. 2. Most-probable (solid) and $\pm 1\sigma$ (broken) m_t curves as a function of $\langle L_{2D} \rangle$. Uncertainties are statistical only. Measured $\langle L_{2D} \rangle$ is overlaid as dashed line.

The second type of systematic uncertainty comes from potential inaccuracies in the size or shape of background L_{2D} distributions. We quantify the uncertainty due to background normalization to be 2.3 GeV/ c^2 by increasing/decreasing the contributions from each background process according to the uncertainties listed in Table I. We estimate the effects of uncertainties in the shape of the background L_{2D} distributions by substituting altered distributions and noting the corresponding shift in m_t . For the W + heavy-flavor background shapes we vary the momentum transfer parameter (q^2) in the calculation. For the non- W shape we substitute a distribution obtained from observed $b\bar{b}$ data. Finally, to estimate the systematic uncertainty due to the distribution used to model the mistag background, we measure the effect on m_t when we alternatively use only the shape derived from the observed data and only the shape derived from MC in place of the data/MC hybrid distribution used in the analysis. We take half the difference between these two determinations as the systematic uncertainty. We add the separate background shape uncertainties in quadrature to arrive at a combined systematic uncertainty of 6.8 GeV/ c^2 .

The final type of systematic uncertainty comes from imperfections of detector simulation of L_{2D} or other, experimentally indistinguishable, disagreements between the $\langle L_{2D} \rangle$ in MC and observed data that may arise from inaccuracies in the simulation of b hadron decays. This uncertainty (4.2 GeV/ c^2) is derived from the error on the $\langle L_{2D} \rangle$ data/MC ratio as discussed above. A total systematic uncertainty of 8.6 GeV/ c^2 is assigned to the measurement. The dominant sources of systematic error are the finite statistics used to derive the $\langle L_{2D} \rangle$ data/MC ratio and the modeling of the L_{2D} distribution due to mistags.

From 456 positive SECVTX tags in 375 events in the lepton + jets sample corresponding to 695 pb $^{-1}$ we measure $\langle L_{2D} \rangle = 0.581$ cm. We draw a vertical line at this $\langle L_{2D} \rangle$ and read off the intersections with the most probable value and $\pm 1\sigma$ confidence interval curves obtained above as illustrated in Fig. 2 to extract a measurement of

$$m_t = 180.7^{+15.5}_{-13.4}(\text{stat.}) \pm 8.6(\text{syst.}) \text{ GeV}/c^2. \quad (2)$$

The L_{2D} distribution of positive tags in selected events, from which the $\langle L_{2D} \rangle$ used to measure m_t is extracted, is shown together with expected contributions from signal and background MC overlaid in Fig. 3. Reasonable agreement between data and MC is observed; a KS test yields a p -value of 16.7%.

We have performed the first measurement of the top-quark mass using the decay length technique. Our measurement is consistent with both the SM expectation and all other Tevatron measurements. Since it has negligible dependence on the jet energy scale and analyzes lepton plus three jet events which are not used by any other m_t measurement, the decay length technique is largely uncorre-

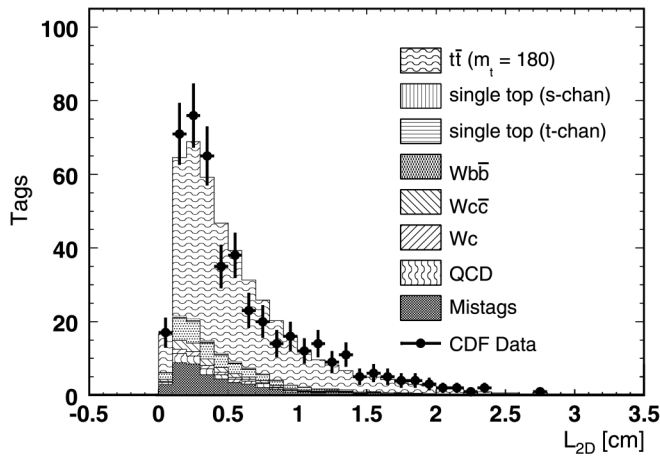


FIG. 3. The L_{2D} distribution of positive tags in selected events. The points are the observed data. Expected contributions from signal and background MC are displayed cumulatively in the histogram. The MC is normalized to the observed data.

lated [23] with other methods. Consequently, while the result presented in this paper is not a competitive measurement of m_t by itself, it helps to reduce the overall uncertainty on m_t when combined with other measurements. In the current world-average value of the top quark mass, $m_t = 171.4 \pm 2.1 \text{ GeV}/c^2$ [24], this measurement contributes at the few percent level to the combined result.

This measurement is statistically limited and its dominant systematic uncertainties are likely reducible. The

precision of this measurement, therefore, will continue to improve. The asymptotic performance of this technique at the Tevatron (and the LHC) are studied in detail in [2]. The current measurement establishes the technique and supports that paper's claim that the decay length method is a useful complement to existing measurements at the Tevatron and beyond.

We thank the Fermilab staff and the technical staffs of the participating institutions for their vital contributions. This work was supported by the U.S. Department of Energy and National Science Foundation; the Italian Istituto Nazionale di Fisica Nucleare; the Ministry of Education, Culture, Sports, Science and Technology of Japan; the Natural Sciences and Engineering Research Council of Canada; the National Science Council of the Republic of China; the Swiss National Science Foundation; the A.P. Sloan Foundation; the Bundesministerium für Bildung und Forschung, Germany; the Korean Science and Engineering Foundation and the Korean Research Foundation; the Particle Physics and Astronomy Research Council and the Royal Society, UK; the Institut National de Physique Nucleaire et Physique des Particules/CNRS; the Russian Foundation for Basic Research; the Comisión Interministerial de Ciencia y Tecnología, Spain; the European Community's Human Potential Programme under contract No. HPRN-CT-2002-00292; and the Academy of Finland.

-
- [1] A. Abulencia *et al.* (CDF Collaboration), *Phys. Rev. Lett.* **96**, 022004 (2006).
- [2] C. S. Hill, J. R. Incandela, and J. M. Lamb, *Phys. Rev. D* **71**, 054029 (2005).
- [3] The lifetime of a top quark is estimated to be $\mathcal{O}(10^{-24})$ seconds.
- [4] D. Acosta *et al.* (CDF Collaboration), *Phys. Rev. D* **71**, 032001 (2005).
- [5] We use a coordinate system where θ is the polar angle to the proton beam, ϕ is the azimuthal angle about this beam axis, and η is the pseudorapidity defined as $-\ln \tan(\theta/2)$. The transverse momentum of a charged particle is denoted as $p_T \equiv p \sin\theta$. The analogously defined energy $E_T \equiv E \sin\theta$, is called transverse energy. Missing transverse energy, \cancel{E}_T , is defined as the magnitude of $-\sum_i E_T^i \hat{n}_i$, where \hat{n}_i is a unit vector in the azimuthal plane that points from the beam line to the i th calorimeter tower.
- [6] The E_T values of jets are corrected for the effects of jet fragmentation, calorimeter nonuniformities and calorimeter absolute energy scale.
- [7] A. Bhatti *et al.*, *Nucl. Instrum. Methods Phys. Res., Sect. A* **566**, 375 (2006).
- [8] A. Abulencia *et al.* (CDF Collaboration), *Phys. Rev. Lett.* **97**, 082004 (2006).
- [9] G. Corcella *et al.*, *J. High Energy Phys.* 01 (2001) 010.
- [10] A. Abulencia *et al.* (CDF Collaboration), *Phys. Rev. D* **74**, 032008 (2006).
- [11] We ascertain the purity by an independent measurement which uses the transverse momentum of the lepton relative to the jet axis in a kinematic fit to distinguish between b and non- b jet contributions to the sample.
- [12] R. K. Ellis *et al.*, *Phys. Lett. B* **78**, 281 (1978).
- [13] B. A. Kniehl, G. Kramer, and B. Potter, *Nucl. Phys.* **B597**, 337 (2001).
- [14] H. L. Lai *et al.* (CTEQ Collaboration), *Eur. Phys. J. C* **12**, 375 (2000).
- [15] P. Avery *et al.*, Cornell Internal Report No. CSN-212, 1985 (unpublished).
- [16] M. L. Mangano *et al.*, *J. High Energy Phys.* 07 (2003) 01.
- [17] This is due to t -channel production which is responsible for $\approx 2/3$ of single-top.
- [18] T. Sjostrand *et al.*, *Comput. Phys. Commun.* **135**, 238 (2001).
- [19] W. M. Yao *et al.* (Particle Data Group), *J. Phys. G* **33**, 1 (2006).

MEASUREMENT OF THE TOP QUARK MASS IN $p\bar{p}$...PHYSICAL REVIEW D **75**, 071102(R) (2007)

- [20] A. Abulencia *et al.* (CDF Collaboration), *Phys. Rev. D* **73**, 032003 (2006).
- [21] A.D. Martin, R.G. Roberts, W.J. Stirling, and R.S. Thorne, *Eur. Phys. J. C* **23**, 73 (2002).
- [22] J. Pumplin *et al.*, *J. High Energy Phys.* 07 (2002) 012.
- [23] We measure correlation coefficients of 0.03, 0.03, and 0.05 between the decay length measurement and the other CDF results in Ref. [24].
- [24] E. Brubaker *et al.* (Tevatron Electroweak Working Group), hep-ex/0608032.